PREDICTION OF HSI NOISE USING A COUPLED EULER/KIRCHHOFF METHOD FOR A HELICOPTER IN HOVERFLIGHT

J. Zibi, O. Rouzaud, C. Polacsek

Office National d'Etudes et de Recherches Aérospatiales

BP72, 92322 Châtillon Cedex, France

Abstract

A coupled multi-bladed Euler/Kirchhoff method has been developed at ONERA to predict the High Speed Impulsive (HSI) noise from helicopter rotors in hover flight with transonic flow. This method has been validated with UH-1H rotor experimental tests. CFD output, provided by the Euler solver WAVES, are transfered to the acoustic Kirchhoff code, KARMA, through an interface programme which computes the pressure and its normal gradients on the Kirchhoff surface, needed to predict the acoustic pressure signature. Aerodynamic computations are in very good agreement with experimental results for the perturbation pressure on the sonic circle. A parametric study of the location of the Kirchhoff surface is performed, from the sonic circle up to the external boundary of the aerodynamic mesh. HSI noise predictions are very stable and accurate for control surfaces located from 1.35 rotor radius up to the last section of the aerodynamic mesh. These satisfactory results are mainly due to the fact that no articifial viscosity is needed in the numerical scheme of WAVES code, and it is concluded that the coupling method WAVES+KARMA is efficient with respect to HSI noise predictions in hover.

Notations

c_0 : speed of sound
M : wind tunnel flow Mach number
R : rotor radius
S_k : Kirchhoff surface
R_k : Kirchhoff surface radius
p : perturbation pressure
p' : acoustic pressure
x_i : observer coordinates in the fixed frame
y_i : source coordinates in the fixed frame
n_i : coordinates of the unit vector $\mathbf{n}$ normal to S_k

d : distance between the source and the observer
τ : emission time
$\beta^2 = 1\text{-}M^2$: Lorentz factor

1 - Introduction

In the last twenty five years, a lot of effort has been devoted to helicopter rotor noise analysis in order to reduce the acoustic nuisance. Impulsive noise, that can occur either at high speed forward flight (HSI noise) or in descent flight (BVI noise), is the most annoying part of noise. This paper focuses on HSI noise analysis, concerning a rotor in hover with transonic flow.

Several ways to describe the HSI noise radiation have been proposed. All involve CFD calculations. The choice of the method is related to the capability of the solver in terms of accuracy, grid extension, and CPU time cost. Three main approaches have been considered. The oldest one is based on the Lighthill Acoustic Analogy (LAA) [1], consisting in a volume integration of the Lighthill's stress tensor. The sound sources are modelled with quadrupoles, requiring second derivatives of local velocities in the non linear domain [2][3][4]. High accuracy requirement for CFD output data and time computation cost for the acoustic volume integration still constitute a major problem not yet solved.

Recent progress in CFD algorithms and computer performances have made a second approach possible. It consists in a full-field CFD calculation, including far-field acoustic waves [5]. This method has been used successfully in hover by Baeder [6][7], but the generation of accurate schemes and local grid refinement strategies, in order to capture the front waves

up to the far-field, remain very complex. For forward flight applications, a direct calculation seems to be even unrealistic, because of CPU cost.

This is the reason why many scientists in the Aeroacoustic community have chosen the Kirchhoff theory [8]. Kirchhoff formulations, reviewed in [9] have been adapted to rotor noise applications in hover [10] and more recently in forward flight [11][12][13], and used by many authors [14][15][16]. This method is very attractive, because it does not require any sound source modelling like in the LAA-based methods. The non linear mid-field CFD solution is propagated up to the control surface enclosing the non linear domain including the acoustic sources. Input data needful to a Kirchhoff code are the perturbation pressure and its time and space derivatives.

This paper presents a coupled multi-bladed Euler/Kirchhoff method, for which each code has been fully developed at ONERA. Though the Kirchhoff method has already been extended to forward flight applications [16], the paper focuses on hover validations. The CFD Euler code (WAVES) [17][18][19][20], and the Kirchhoff code (KARMA) are described, more particularly the scheme and the grid generation used. The output data interface needful to KARMA is presented in detail. The validity of the method is then tested on UH-1H rotor hover tests [2]. Comparisons with experimental data are made. Influence of CFD grid refinement and control surface location are also discussed.

This work is performed in the framework of a french-german ONERA-DLR cooperation on helicopter rotors aerodynamics and aeroacoustics.

2 - Numerical solution procedures

2.1 - Euler code

Governing equations

Previous works [6][7] tend to show that the numerical study of the HSI noise can be correctly modelled by the Euler equations. The shocks are well represented and these equations properly model the non-linear propagation of the acoustic waves as well as the convection of entropy and vorticity. Furthermore,

Navier-Stokes computations require a fine grid to resolve the boundary layer and are far more expensive. Thus, the WAVES code described in this paper solves the 3D compressible Euler equations and these equations are transformed in a blade attached rotating frame [20]. In this reference frame, the equations are formulated in terms of absolute velocities.

Numerical method

A detailed description of the ONERA Euler WAVES code for hovering rotors is given in [20][21]. The Euler equations in integral form are discretized on a curvilinear structured grid using a cell-centered finite-volume approach.

The basic Euler solver is divided in an explicit stage of second order accuracy which is an original multidimensional version of the Lax-Wendroff scheme [17] and an implicit stage of order of the truncation error of the global scheme [19]. The implicit stage is split into each space direction using the ADI factorization method, and simplified by replacing the block matrices by their spectral radii (Scalar Approximation Factorization) [18].

In this method, the intrisic dissipation is due to the second order term of the explicit stage and increases with the CFL number. This method works without artificial viscosity in the transonic regime.

Concerning the boundary conditions, the slip condition is prescribed on the blade surface and the pressure is obtained from the discrete form of the momentum equations in order to get a conservative approximation of the normal momentum equation. For the far-field and the hub boundaries, the boundary conditions are given by using the concept of characteristic variables.

Grid generation

As suggested by Baeder [6], the grid is clustered not only on the blade surface but also near the curve predicted by the linear characteristic theory. By this mean, pressure perturbations propagating from the blade towards the far-field are expected to be correctly captured. A view of the rotor plane shows the specific clustering of the coarse grid used in the calculations for a tip Mach number of 0.90 (Fig. 1). Besides, this figure also shows that a periodicity condition is ensured between the upstream

and downstream planes, allowing the computations of multibladed rotors in hover. No linear interpolation between the two planes is required as each point of the upstream plane corresponds to a point in the downstream plane. The periodicity condition improves the accuracy of the computations. In this article, all the results have been obtained for multibladed rotors in hover.

The 3D grid is built in three stages. In a first step, the blade sections and the sections out of the blade are defined and their locations along the spanwise axis are given. In the next stage, two-dimensional C-grids are built for each section. Finally, the planes are bent and the periodicity condition is prescribed. Out of the blade, each section lies at a constant radial distance from the rotational axis. Fig. 2 shows a general view of the grid.

2.2 - Kirchhoff code

KARMA code computes the Kirchhoff integral according to the formulation in [13]:

$$p'(x,t) = \frac{1}{4\pi} \int_{S_k} \left[\frac{1}{d} \left(-M^2 \frac{\partial p}{\partial n_1} + \frac{\partial p}{\partial n} - \beta^2 \frac{p}{d^2} n_i(x_i - y_i) - \frac{1}{c_0} \left(\frac{n_i(x_i - y_i)}{d} + Mn_1 \right) \frac{\partial p}{\partial \tau} \right) \right]_\tau dS$$

For hover cases, this equation can be written in the conventional form [10] :

$$p'(x,t) = \frac{1}{4\pi} \int_{S_k} \left[\frac{1}{d} \left(\frac{\partial p}{\partial n} - \frac{p}{d^2} n_i(x_i - y_i) - \frac{n_i(x_i - y_i)}{c_0 d} \frac{\partial p}{\partial \tau} \right) \right]_\tau dS$$

In this formulation, the Kirchhoff surface S_k is a fixed cylinder surrounding the rotor, the top and bottom surfaces being neglected. The input data required on this cylinder are the pressure and its normal gradient. These data are provided by an interface procedure between the aerodynamic WAVES code and the acoustic KARMA code.

As the Kirchhoff surface is held fixed, a 2D bilinear interpolation is used to transfer CFD output data for which grid points are not equally spaced in azimuth to the fixed grid, for which a constant azimuthal spacing is used.

KARMA code computes the acoustic pressure time histories for one or several observers, corresponding to microphone locations in the wind tunnel frame. The source terms in the Kirchhoff integral are evaluated at the retarded time,τ, for each position of the blade, with respect to the azimuthal spacing of the acoustic grid. For each emission time, the observer time is deduced from the retarded time equation, so that no quadratic equation resolution is needed. The azimuthal spacing of the Kirchhoff fixed grid is equal to 1024 points per rev. The vertical spacing is chosen to correspond to the aerodynamic one at the trailing edge of the blade. The integration domain has an extension from -50° to 50° in the azimuthal direction and an extension of one rotor radius ($\pm$ 1R) in the vertical direction.

2.3 - Interface procedure

The aerodynamic data needed by the Kirchhoff equation are the pressure and the normal gradient of the pressure on the Kirchhoff surface. The pressure is calculated using the following state relation :

$$p = (\gamma - 1)\rho(E - 1/2\mathbf{q}^2)$$

where ρ is the fluid density, $\mathbf{q}$ the absolute velocity, E the specific total energy obtained by the WAVES calculation.

An interface programme has been developed to compute the perturbation pressure and its normal gradient on the Kirchhoff surface. The pressure gradient is the most contributing term to far-field noise radiation, and thus requires a careful calculation. For this purpose, an efficient and accurate method based on the finite volume formulation is used to calculate these terms :

$$\frac{\partial p}{\partial \mathbf{n}} = \mathbf{grad}p.\mathbf{n} \quad \text{by definition}$$

with $\mathbf{gradp} = \dfrac{1}{V} \displaystyle\int_{\text{cell boundaries}} \text{pndS},$

V being the volume of a cell, ndS the outward normal surface vector .

3 - Applications

3.1 - Experimental conditions

This coupled Euler/Kirchhoff method is applied to predict the HSI noise generated by the UH-1H model rotor of the US Army. This rotor is untwisted, has two rectangular blades equiped with the NACA0012 airfoil; the blade aspect ratio is 13.71. The flight configuration is a hover nonlifting case for a tip Mach number of 0.90. Delocalization phenomenon occurs allowing pressure perturbations to be propagated in the far-field.

The different observer positions correspond to microphones located at 2.18 and 3.09 rotor radius from the rotor hub, in the rotor plane and in the advancing direction. The experimental acoustic sampling rate is 2048 points per rotor revolution, equally time spaced.

3.2 - Computational parameters

A two-bladed Euler simulation is performed in a computational domain representing half of the whole domain, the periodicity condition being respected in the upstream and downstream planes. Three meshes with an increasing number of points are generated in order to study the influence of grid refinement on WAVES calculations. These meshes are generated from a coarse grid of 131 points in the chordwise direction, 42 points in the spanwise direction and 22 points in the normal direction, i.e. 121 044 points in total. This grid is refined to obtain a medium grid of (221x70x32), i.e. 495 040 points, and a fine grid of (285x90x42), i.e. 1 077 300 points.

Control surface position is one of the most influent parameter on Kirchhoff predictions. Thus, an analysis of acoustic results with respect to the position of the Kirchhoff surface has been performed for the medium grid, for several positions from the sonic circle up to the external boundary of the mesh, in order to study the influence of the non-linear

contributions. As the chosen test case is non lifting, the Kirchhoff surface is limited to half a cylinder.

4 - Experimental and theoretical comparisons

4.1 - Aerodynamic results

The pressure distributions for the three different meshes for six spanwise sections are shown in Fig. 3. Unfortunately, experimental data are not available. As the mesh is refined, the location of the shock wave is moving to the leading edge, and the structure of the shock is getting steeper. The WAVES code has the advantage not to use artificial viscosity, so that numerical dissipation is reduced. Convergence is obtained after about 8500 iterations for the coarse and medium grid calculations. The fine grid requires more iterations.

Fig. 4 shows the iso-Mach contours in the rotor plane, upper surface. The delocalization phenomenon is clearly displayed. It can be noticed that the structure of the shock is defined more accurately when the grid is refined. This figure also shows how the mesh is following the propagation of the perturbation in the rotor plane, as a result of the generation of an adapted mesh.

Perturbation pressure provided by WAVES code on the sonic circle (located at 1.11 rotor radius) is compared to experimental data in Fig. 5. Two parameters are very important for accurate acoustic computations, which are the determination of the negative peak, and more particularly the recompression slope. The coarse grid does not provide very accurate results, since the minimum pressure peak is underpredicted. The results are becoming more accurate when the grid is refined. The correlation with the experimental slope is very satisfactory for the medium and the fine grids calculations. We can also notice that a small oscillation occurs experimentally just after the recompression. Similar oscillation appearing on the computed signature can be related to this phenomenon.

4.2 - Acoustic results

Analysis of WAVES computation results

A parametric study on the location of the Kirchhoff surface is done for the medium grid. In order to study the influence of the non linear effects, several positions from 1.15 up to 1.7 rotor radius, corresponding to the external boundary of the aerodynamic mesh, are chosen. Fig. 6 shows the perturbation pressure for these different positions, the origin of the phase being taken for the first position at 1.15 rotor radius. Unfortunately, no comparisons with experimental data are available. It can be noticed that the amplitude of the negative peak is rapidly decreasing from 1.15 up to 1.35 rotor radius and the recompression slope is getting steeper. The symmetrical shape of the pressure signature at 1.15 rotor radius is due to non-linear effects which tend to sharpen the compression wave and to flatten the expansion wave up to the vicinity of the sonic cylinder (1.11 rotor radius) [7]. Beyond this region, non-linear effects are decreasing, making the shape of pressure signature getting more asymmetrical. From 1.35 up to 1.7 rotor radius, the shapes of pressure signatures, in terms of slope and recompression peak, tend to be stabilized. The negative peak is decreasing roughly following an $1/r^2$ acoustic near-field attenuation which supposes the linear domain is reached. This regular evolution up to the boundary of the mesh seems to demonstrate that WAVES solver is able to propagate shock waves without noticeable dissipation. All these remarks will be helpful to analyse the Kirchhoff results.

Analysis of KARMA computation results

The Kirchhoff code has been run using the CFD input data relative to each control surface location. Computed acoustic signatures relative to the microphone located at 3.09 rotor radius are plotted in Fig. 7, the radius of the Kirchhoff surface varying from 1.15 up to 1.5 rotor radius. The evolution of far-field acoustic pressure is in accordance with WAVES results obtained above on the different Kirchhoff surfaces. From 1.15 up to 1.25 rotor radius, acoustic pressure signatures provided by KARMA have a smooth relative peak amplitude and rather symmetrical shape. For Kirchhoff surface radii greater than 1.25 rotor radius, as explained before, the Kirchhoff surface tends to enclose the non linear regions, making the far-field acoustic signature to become asymmetrical, and the recompression to get sharper. The same signatures are compared to experiment in Fig. 8. The correlation is very satisfactory beyond 1.35 rotor radius, despite a very small increase of the negative peak amplitudes, probably due to numerical errors. Computed signatures for 1.35 rotor radius are enlarged and compared to experiment in Fig. 9, for both microphones. The predicted sound pressure levels (indicated in dB in Fig. 9) are very close to experimental data, which confirms the accuracy of the method. All these results are summarized in Fig. 10, showing the differences between computed and experimental pressure levels as a function of the Kirchhoff surface radius. From 1.35 rotor radius up to the mesh boundary, WAVES+KARMA provides stable and accurate predictions, with pression level deviations less than ± 0.3dB.

5 - Conclusions

A coupled Euler/Kirchhoff method has been developed to predict the HSI noise for a helicopter rotor in hover flight with transonic flow. The first step consists in generating an adapted mesh in order to correctly capture the propagation of the pressure perturbations. The aerodynamic data are then transmitted through an interface programme which calculates the pressure and its normal gradient on the Kirchhoff surface, needed by the Kirchhoff KARMA code to predict the acoustic pressure signature.

This methodology has been applied to predict the HSI noise generated by the UH-1H rotor in hover, for a tip Mach number of 0.90. Aerodynamic computations are in very good agreement with experimental results for medium and fine grid calculations. In particular, the perturbation pressure on the sonic circle is quite well predicted. A parametric study relative to the Kirchhoff surface location with respect to the domain of validity of the methodology has been performed. HSI noise predictions are very stable and accurate for control surface located from 1.35 rotor radius up to the mesh boundary (1.7 rotor radius). This very satisfactory result is mainly due to the fact that the numerical scheme used in the WAVES code does not require any artificial viscosity, which is of course

determinant for an efficient use of a Kirchhoff method. These predictions, comparable to Baeder's results, clearly demonstrate the robustness of both Euler and Kirchhoff ONERA codes, with respect to HSI noise calculations in hover. The next step of the prediction of HSI noise will be to apply this methodology for forward flight configurations.

6 - References

[1] Lighthill, M.J.,"On Sound Generated Aerodynamically", Philosophical Transactions of the Royal Society, No. A564, 1952.

[2] Schmitz, F.H., and Yu, Y.H.,"Transonic Rotor Noise - Theoretical and Experimental Comparisons", Vertica, Vol. 5(1), pp. 55-74, 1981.

[3] Prieur, J.,"Calculation of Transonic Rotor Noise Using a Frequency Domain Formulation", AIAA Journal, Vol. 26(2), pp. 156-162, February 1988.

[4] Farassat, F., and Tadghighi, H., "Can Shock Waves on Helicopter Rotors Generate Noise ? A Study of Quadrupole Sources", 46th AHS Annual Forum, Washington D.C., May 1990.

[5] Srinivasan, G.R., and Baeder, J.D., "Recent Advances in Euler and Navier-Stokes Methods for Calculating Helicopter Rotor Aerodynamics and Acoustics", 4th International Symposium on Computational Fluid Dynamics, Davis, California, 1991.

[6] Baeder, J.D., "Euler Solutions to Nonlinear Acoustics of Non-Lifting Hovering Rotor Blades", 16th ERF, Glasgow, Scotland, September 1990.

[7] Baeder, J.D., Gallman, J.M., and Yu, Y.H., "A Computational Study of the Aeroacoustics of Rotors in Hover", 49th AHS Annual Forum, Saint-Louis, Missouri, May 1993.

[8] Morgans, R.P., "The Kirchhoff Formula Extended to a Moving Surface", Philosophical Magazine, 9, s. 7, No. 55, pp. 141-161, 1930.

[9] Lyrintzis, A.S., "Review: The Use of Kirchhoff's Method in Computational Aeroacoustics", Journal of Fluids Engineering, Vol. 116, pp. 665-676, December 1994.

[10] Pierce, A.D., "Acoustics: An Introduction to its Physical Principles and Applications", Mc Graw-Hill, New-York, 1981.

[11] Morino, L., "Mathematical Foundations of Integral Methods", Computational Methods in Potential Aerodynamics, ed. Springer-Verlag, New-York, pp. 271-291, 1985.

[12] Farassat, F., and Myers, M.K., "Extension of Kirchhoff's Formula to Radiation from Moving Surfaces", Journal of Sound and Vibration, Vol. 123(3), pp. 451-460, 1988.

[13] Polacsek, C., Prieur, J., "High-Speed Impulsive Noise Computations in Hover and Forward Flight Using a Kirchhoff Formulation", 16th AIAA Aeroacoustics Conference, Munich, Germany, June 1995.

[14] Strawn, R.C., and Biswas, R., "Computation of Helicopter Rotor Acoustics in Forward Flight", 19th Army Science Conference, Orlando, Florida, June 1994.

[15] Kuntz, M., Lohmann, D., Lieser, J.A., Pahlke, K., "Comparisons of Rotor Noise Predictions Obtained by a Lifting Surface Method and Euler Solutions Using Kirchhoff Equation", 16th AIAA Aeroacoustics Conference, Munich, Germany, June 1995.

[16] Polacsek, C., Costes, M., "Rotor Aeroacoustics at High-Speed Forward Flight Using a Coupled Full Potential/Kirchhoff Method", 21st ERF, Paper No II.6, Saint Petersburg, Russia, September 1995.

[17] Lerat, A., Sidès, J., "Efficient Solution of the Steady Euler Equation with a Centered Implicit Method", Num. Meth. Fluid Dyn. III, R.K.W. Morton and M.J. Baines Eds., Clarendon Press, Oxford, p.65-86, 1988.

[18] Lerat, A., Sidès, J., Daru, V., "An Implicit Finite-Volume Method for Solving the Euler Equations", Lecture Notes in Physics, Vol. 17, ed. Springer-Verlag, pp. 343-349, 1982.

[19] Lerat, A., "Implicit Methods of Second-Order Accuracy for the Euler Equations", AIAA Paper 83-1925, 1985.

[20] Boniface, J.C., Sidès J., "Numerical Simulation of Steady and Unsteady Euler Flows

Around Multibladed Helicopter Rotors", 19th ERF, Cernobbio, Italy, September 1993.

[21] Raddatz, J., Rouzaud, O.,"Calculations of Multibladed Rotors in Hover Using 3D Euler Methods of DLR and ONERA", 21st ERF, Paper II.6, Saint Petersburg, Russia, September 1995.
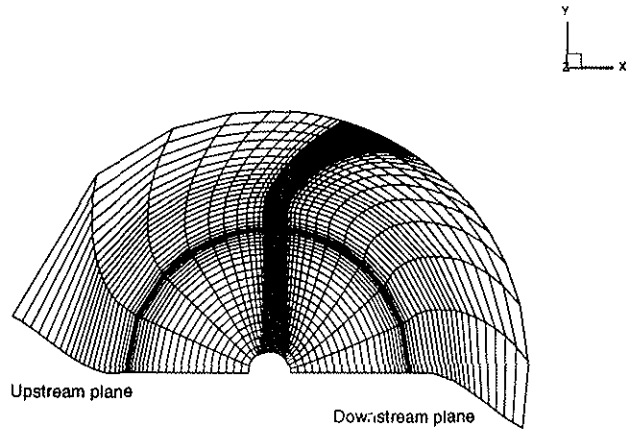
Fig. 1: View of the adapted mesh in the rotor plane
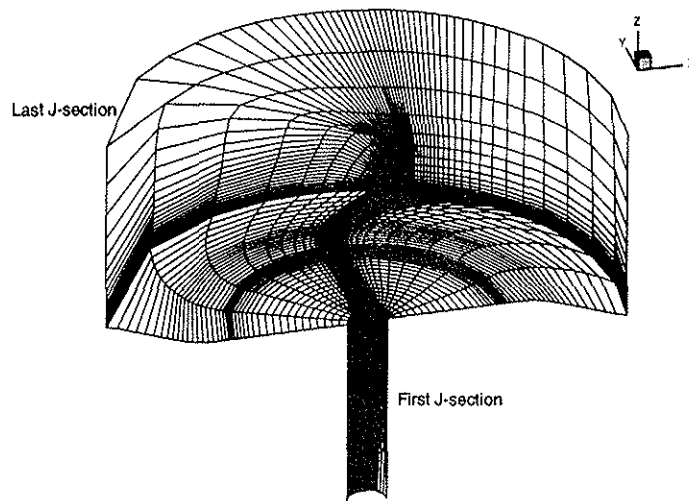
Fig. 2: General view of the mesh
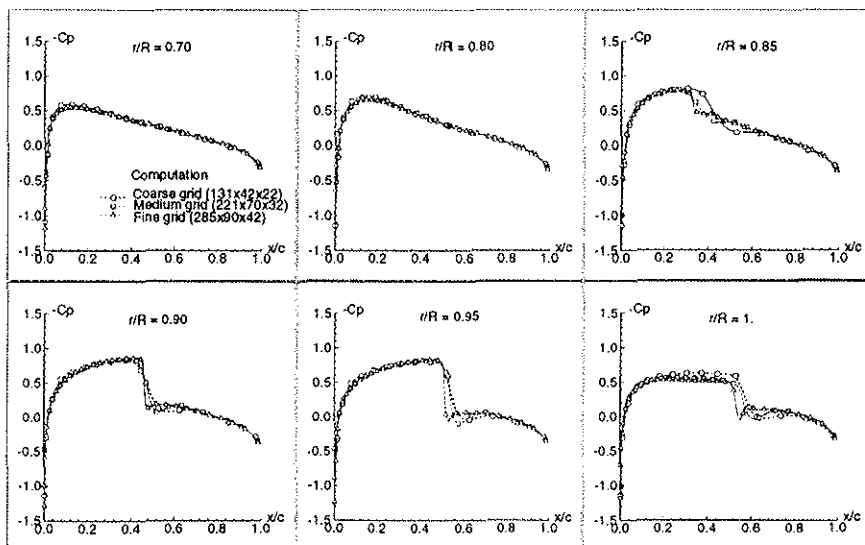
Fig. 3: Influence of grid refinement on pressure distributions

Calculation on coarse grid   Calculation on medium grid   Calculation on fine grid
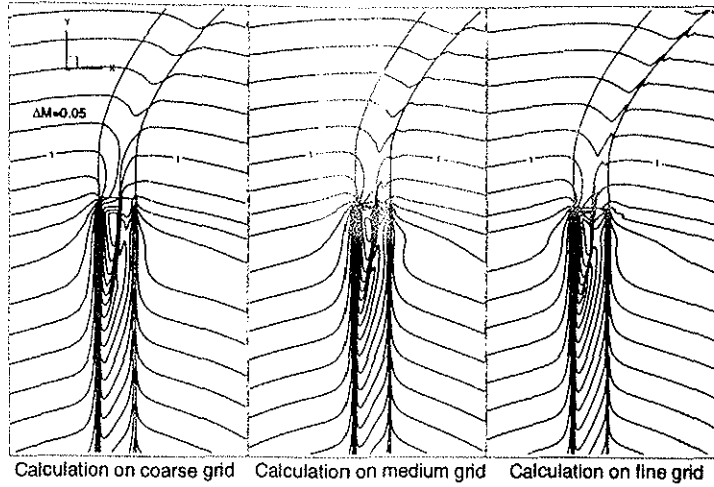
Fig. 4: Influence of grid refinement on iso-Mach contours in the rotor plane, upper surface
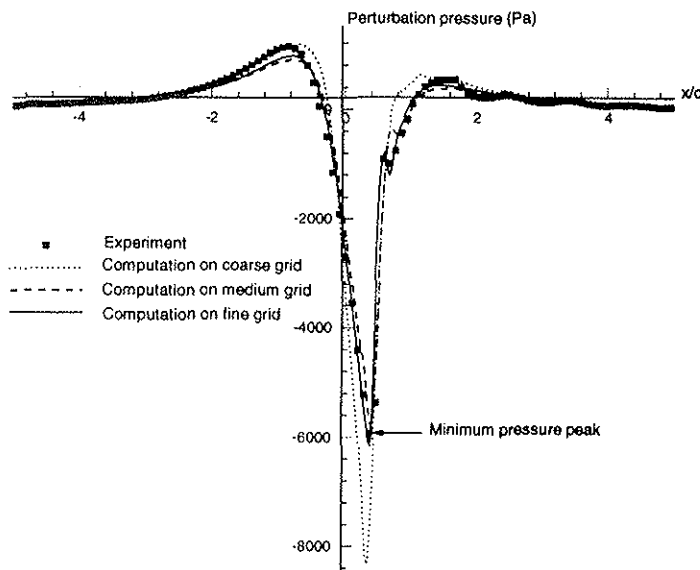
Fig. 5: Experiment/Computation comparisons of perturbation pressure on the sonic circle
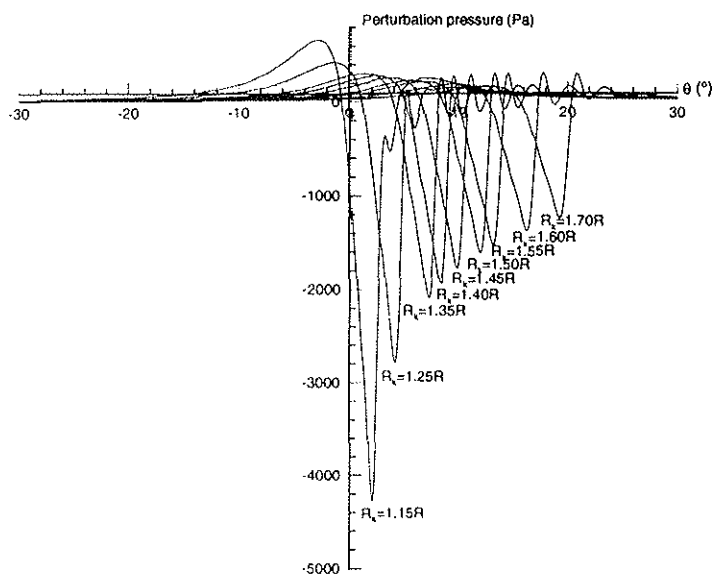
Fig. 6: Influence of Kirchhoff surface location on perturbation pressure - Medium grid
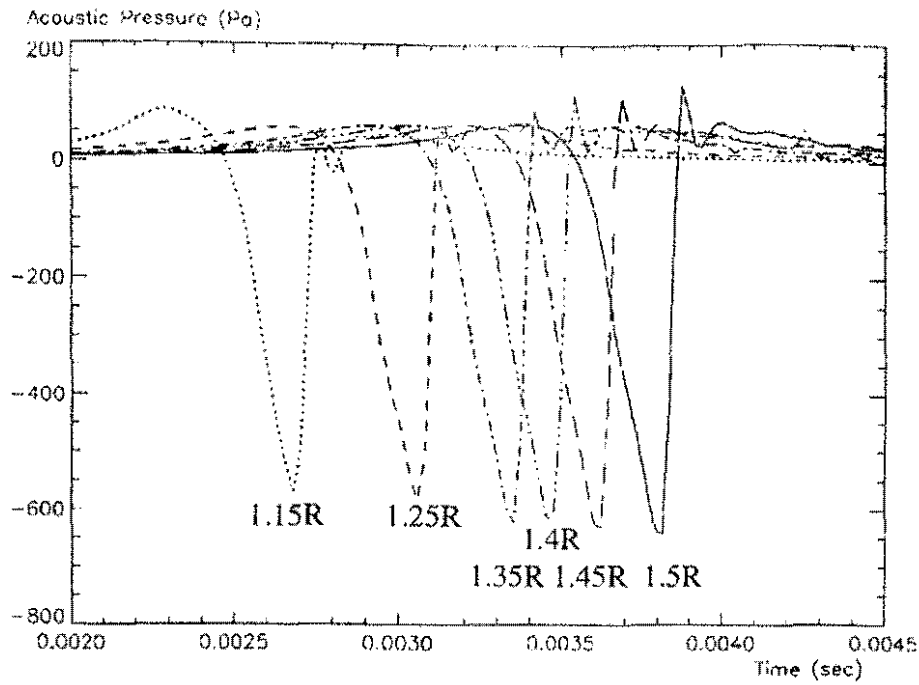
Fig. 7: Influence of Kirchhoff surface location on acoustic pressure - Medium grid - Mic: 3.09R
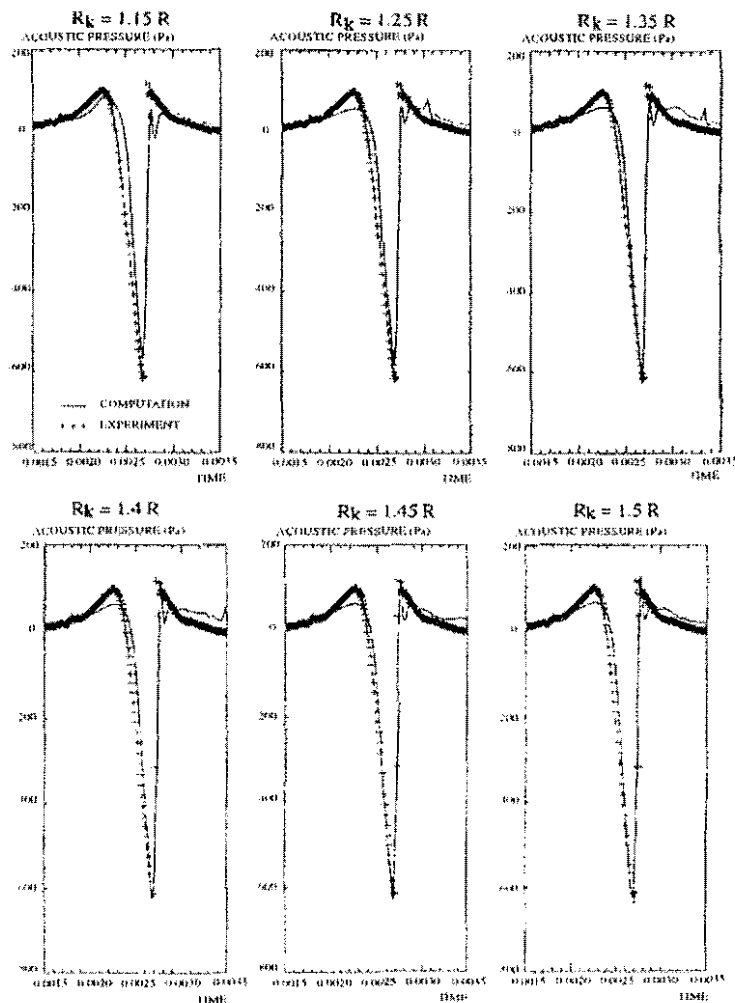
Fig. 8: Experiment/Computation comparisons of acoustic pressure signature for each Kirchhoff surface location - Medium grid - Mic: 3.09R
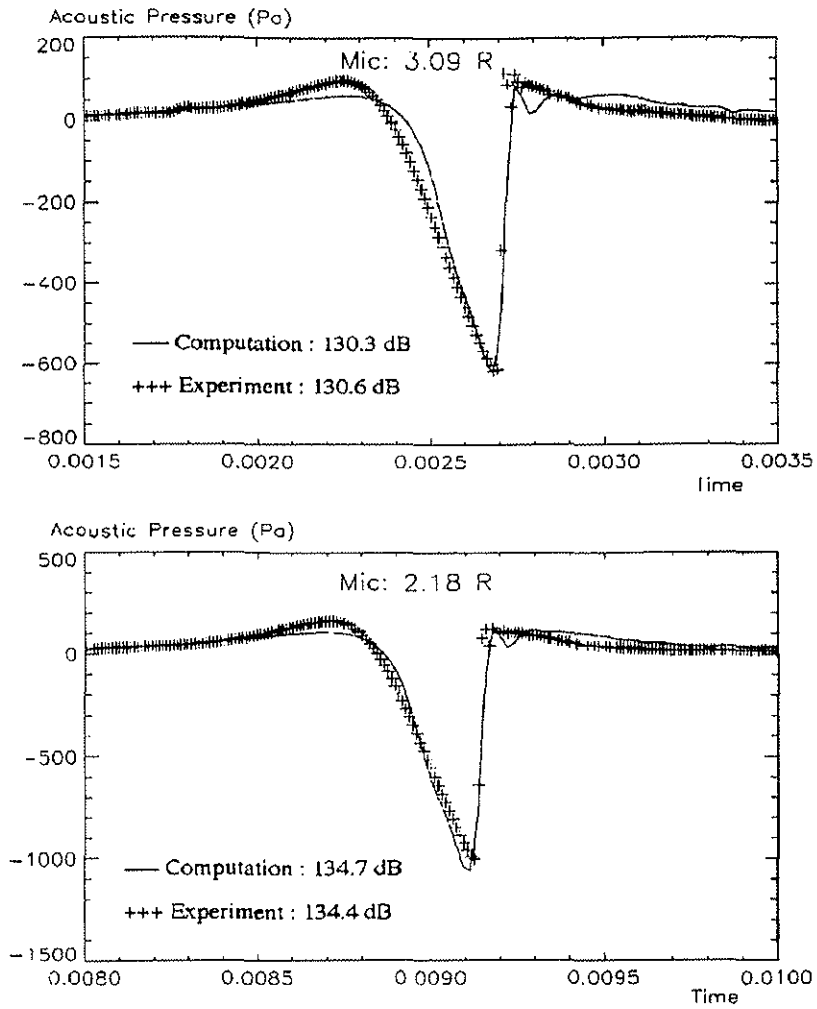
Fig. 9: Experiment/Computation comparisons of acoustic pressure signature on the Kirchhoff surface $R_k=1.35R$
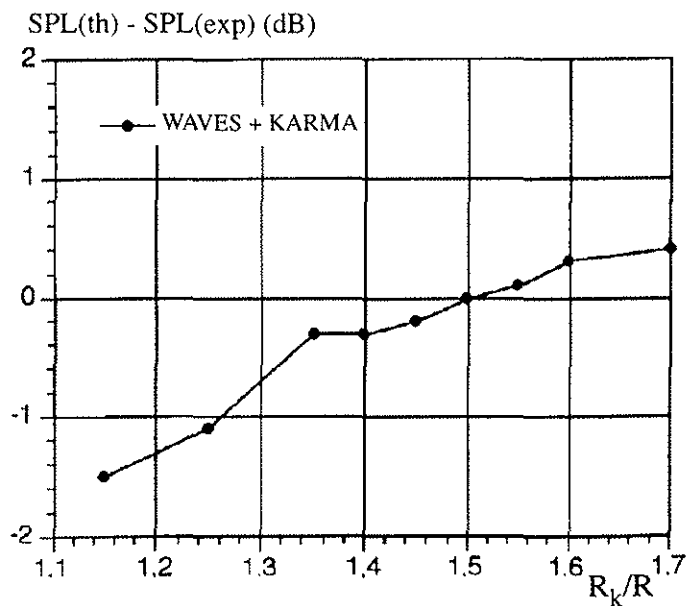
Fig. 10: Theoretical and experimental pressure level deviations with respect to Kirchhoff surface radius - Medium grid - Mic: 3.09R